GeoResJ 9–12 (2016) 54–66

Contents lists available at ScienceDirect

GeoResJ

journal homepage: www.elsevier.com/locate/georesj

# Holocene multistage massive ice, Sabettayakha river mouth, Yamal Peninsula, northwest Siberia

Yurij Vasil'chuk[a,*], Nadine Budantseva[a], Alla Vasil'chuk[a], Julia Chizhova[a], Yevgeny Podborny[b], Jessica Vasil'chuk[a]

[a] Geography Department, Lomonosov Moscow State University, Leninskie Gory, 119991 Moscow, Russia
[b] Center of Hydroecological Research, Nalichnaya street, 16/A, 199406, Saint-Petersburg, Russia

ARTICLE INFO

*Article history:*
Received 1 September 2016
Accepted 4 September 2016
Available online 6 September 2016

ABSTRACT

Massive ground ice of Holocene age occurs in multiple boreholes near the Sabettayakha River mouth, on the coast of the Gulf of Ob (Ob Bay), Yamal Peninsula, northwest Siberia. The multistage massive-ice bodies are up to 5.7 m thick and occur in Holocene sediments of modern floodplain and the first terrace of the coastal lagoon. Massive-ice bodies and cryopegs occur at three to four depths. According to stable isotope analyses, the multistage massive ice bodies formed syngenetically during the freezing of water-saturated sediment, under intensive cryogenic fractionation. Very negative values of $\delta^2$H (up to −199.7 ‰) and $\delta^{18}$O (up to −26.48 ‰) for the massive ice are unique not only for Holocene ground ice of Yamal Peninsula, but also for Late Pleistocene ice of northwest Siberia. The ratio of the chloride and sulfate anions, pollen spectra and presence of algae in three different types of massive ice near the Sabettayakha River mouth suggest that (1) vertically layered brown ice formed during freezing of water-saturated sands of the Ob Gulf; (2) brown non-laminated ice formed as a result of freezing of sublake talik water; and (3) white ultra-fresh ice also formed from lake and river water.



## 1. Introduction

Massive ice in permafrost is one of the most important indicators of global and climate change. It is considered that the relics of Quaternary glaciation are preserved as ice fragments in permafrost in large areas of the polar regions. However, intrasedimental ice bodies are often found in these areas and are usually of Holocene age. They may occur in the centre of pingos, where they are well marked in the modern landscape. Otherwise, tabular bodies of massive ice may form by freezing of the water table, and such ice bodies are often not apparent in the relief. Nowadays it is possible to claim that the widely distributed buried ice bodies are glaciation relics in Antarctica, Greenland and Arctic Canada, where modern ice sheets or glaciers exist today. In areas of strongly saline Quaternary marine deposits of northwest Siberia, however, the chance to detect buried relics of glaciers is very small. In order to distinguish between buried and intrasedimental ice bodies it is possible to compare them with modern analogs or massive ice enclosed in permafrost whose origin is known. Massive ice within permafrost marine and lagoon-marine sediments where there were no any glaciation in the Holocene [25] can be an example of massive ice of non glacial origin. The study of the composition and structure of massive-ice bodies in such deposits i may allow us to define the basic indicators for distinguishing intrasedimental formation of ice bodies and glaciation relics. Combinations of massive-ice bodies of different structure and composition in Holocene deposits are particularly interesting for paleogeocryological reconstructions because they show the variety of ice formation even in relatively homogeneous environmental and climatic conditions. The uniqueness of the Holocene permafrost in the estuary of Sabettayakha River, on the Yamal Peninsula, lies in the fact that freshwater conditions of the Ob River are replaced periodically by brackish conditions related to the drift of the Kara Sea salt water, which often has a temperature below 0 °C during the cold season. This shift of freshwater and brackish-water regime is likely to trigger the formation of intrasedimental ice bodies or burial of fast ice during the Holocene and in modern conditions and it may be marked in the Holocene deposits by cryopeg lenses and horizons.

Pleistocene bodies of massive ice have often been interpreted as buried glacier ice [2,14,15,24]. Holocene massive ice within subarctic lowlands in northwest Siberia, however, cannot be buried glacier ice because there is no evidence of Holocene glaciers there. The last extensive glaciation of this area is thought to have been during the early Weichselian, about 90–80 ka [1,28]. Thus, Holocene massive ice in northwest Siberia may have formed

* Corresponding author.
*E-mail address:* vasilch_geo@mail.ru (Y. Vasil'chuk).

http://dx.doi.org/10.1016/j.grj.2016.09.002

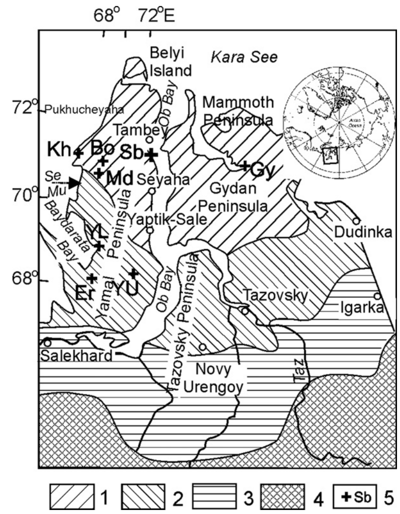


**Fig. 1.** Map showing permafrost distribution in northwest Siberia and the locations of the massive-ice bodies: 1 – 2 – continuous permafrost: 1 – mean ground temperatures lower than −5 °C, 2 – mean ground temperatures from −3 to −5 °C; 3 – 4 – discontinuous permafrost: 3 – mean ground temperatures from −1 to −3 °C; 4 – mean ground temperatures from −0 to −1 °C; 5 – massive ice localities: Kh – Cape Kharasavey, Bo – Bovanenkovo gas-condensate field, Sb – Sabettayakha River, Md – Mordyyakha River, YL – lower reaches of the Yuribey River, YU – upper reaches of the Yuribey River, Er – Erkutayaha River, Oy – Oyuyakha River, Gy – lower reaches of the Gyda River. Also shown also is the Seyaha River (Mutnaya) mouth – Se Mu.

intrasedimentally by ice segregation or injection of water under high pressure or by burial of ice floes and ice feet.

Massive-ice bodies of Holocene age in northwest Siberia are rare in comparison with those of Pleistocene age. Holocene massive ice has been reported beneath the floodplain of the lower reaches of the Sabettayakha River, northeast Yamal Peninsula (Fig. 1; [30]). The ice was about 0.5 m thick, had a vertical column texture and occurred in very icy sand at a depth of 3–4 m. It was interpreted as buried river ice. Massive-ice bodies occur elsewhere on the Yamal Peninsula: in the floodplain sediments of the Yuribey River [16], within the first terrace near Kharasavey settlement [4], in the bottom sediments of Baydarata Bay and the Kara Sea [12], and in the floodplain and channel sediments of the Seyaha River (Mutnaya) [34].

The aim of this paper is to interpret the origin of multiple bodies of massive ice within the Holocene lagoon-marine floodplain of Ob Bay and the first lagoon-marine terrace near the Sabettayakha River mouth, Yamal Peninsula (Fig. 1), based on the results of stratigraphic, isotopic geochemical and pollen analyses of the massive ice.

## 2. Study site

The study site is located in a coastal area comprising arctic tundra with many lakes and swamps. The first Holocene lagoon-marine terrace contains extensive flat-floored alases at an altitude of 5–12 m above sea level (a.s.l.) and includes complex Holocene lagoon-marine sediments (see supplementary material Fig. S1a). The modern lagoon-marine floodplain (tidal marsh) of the Ob Bay is composed of Holocene alluvial-marine deposits (see supplementary material Fig. S1b). On the surface of the geomorphological levels a recent ice-wedge polygon network is prevalent. The upper part of the lagoon-marine floodplain and the first and second lagoon-marine terraces comprise mainly sands (more than 50% of total sediments); whereas the lower parts often comprise loam. Loam constitutes slightly more than 20% of the permafrost section examined and sandy loam about 12% of it (see supplementary material Fig. S2). Silt is common in the upper part of the section, where sediments of the modern river bay (or lakes on the floodplain) are water-saturated, and plant residues and humus are well preserved.

The Holocene age of the first lagoon-marine terrace on the north of Yamal Peninsula which accumulated simultaneously along Yamal Peninsula coast is inferred from a number of $^{14}$C ages from the lower part of the first terrace near the Pukhucheyakha River mouth, on the northwest coast of the peninsula [36,43]. At the same place buried wood from a depth of 7 m provided an age of 8250 ± 80 years BP (LU-1139) and wood from a depth of 4.5 m provided one of 6580 ± 60 years BP (LU-1138). $^{14}$C ages of 8500 ± 120 years BP (LU-1151) and 8960 ± 140 years BP (MSU-816) obtained from basal peat from the first marine terrace of the Belyi Island and from peat at 5 m depth in the first lagoon-marine terrace of the Ob Bay near Yaptik-Sale settlement, respectively (Fig. 1).

Prevailing landscapes in the study area are alluvial and marine low plains, with dwarf-shrub tundra vegetation.

To the north, near the Tambey (Fig. 1) the vegetation comprises different types of lichens, mosses, tundra herbs and in some places dwarf willow. Sedge-hypmun polygonal bogs on peaty and clay soils are widespread. In the subfossil pollen spectra, sedge pollen dominates (5.2–16.8%) as well as pollen of cereals (3.5–12%), indicating a dominance of these species in a plant communities. Pollen of other species, as a rule, occurs rarely, often without corresponding to their role in plant communities. Subfossil pollen spectra are characterized by a high content of wind-transported pollen of *Pinus sylvestris* (to 8–9%) and *P. sibirica* (to 10–12%). Pollen of fir (*Picea*) does not exceed 2%, dwarf birch is up to 18%, and *Alnus (Duschekia*) is less than 5% [43].

### 2.1. The holocene history of the study site

The study area was unglaciated during Last Glacial Maximum. There was limited extension of the ice sheet into the Kara Sea. The eastern limit of the late Weichselian Eurasian ice sheet is between Novaya Zemlya and the Yamal Peninsula [5,35,40]. Studies along the lowlands of the eastern Kara Sea provide equivocal evidence for glaciation by a large ice sheet in the late Weichselian, but support ice-free conditions in large areas, and Pleistocene flora, mammals, and humans survived throughout the late Weichselian into the Holocene. Thus, the late Weichselian glacier extent characterized by expansion of valley glaciers in the Ural Mountains [1] and probably limited extension of ice caps on Severnaya Zemlya [28].

According to Premke-Kraus [21] the earliest Holocene (ca. 9600 – 9000 cal. BP) was the warmest phase and marks probably the termination of the Holocene thermal maximum (HTM) in the coastal Kara Sea. The shrub tundra was displaced by the forest tundra, with a stronger contribution of tree birch. The sparse herbaceous pollen suggests relatively low species diversity at this time. As a consequence of the rising sea level and groundwater table due to permafrost degradation, floodplains developed along the lowlands. Except for short-term cold events, favorable climate conditions have prevailed since 9000 cal. BP, but a gradual deterioration is indicated. This led at first to better conditions for tree growth such as fir and spruce due to milder winters. However, at ca. 7400, 5700 and 3800 cal. BP, the stepwise increases of herbaceous pollen such *Artemisia* and Poaceae pollen and the decrease of *Picea* pollen, respectively indicate climate deterioration. More pronounced, at ca. 2000 cal. BP, pollen spectra indicate a displacement of the boreal forest by Arctic tundra communities and the establishment of modern conditions.

The climate of the area is characterized by a long cold winter with stable snow cover and a brief cool summer. The period with positive average daily air temperature is up to 109 days. The period with average daily air temperature below 0 °C ranges from

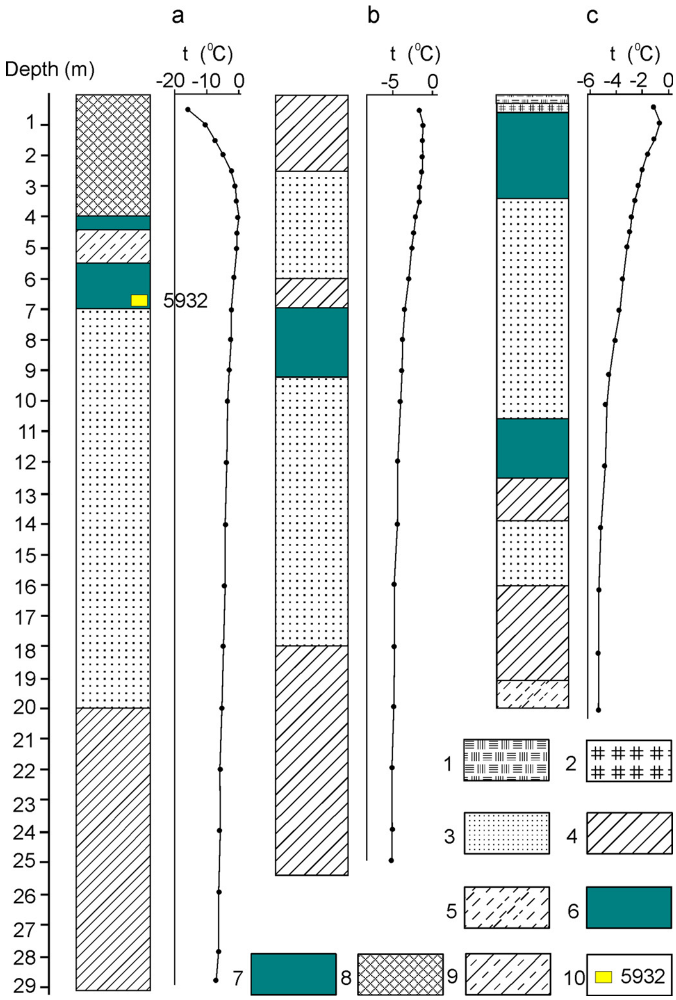


**Fig. 2.** Lithology and ground temperatures (measured in 2014) of floodplain and first lagoon-marine terrace containing massive-ice bodies near the Sabetta settlement, northeast Yamal Peninsula: a – borehole 12, b – borehole 17, c – borehole 42: 1 – moss and plant cover; 2 – sand; 3 – peat; 4 – loam 5 – sandy loam; 6 – white transparent, horizontal layered ice; 7 – brown vertical layered ice; 8 – artificial soil; 9 – black silt; 10 – direct AMS radiocarbon age of ice.

256 to 265 days per year, from October to May. Air temperatures above 0 °C generally commence in the first half of June. The earliest date for a sustainable transition at 0 °C in the spring, recorded at Tambey station, is in mid-May, but the transition mostly occurs in late May to late June. The mean annual air temperature is −10.2 °C.

Permafrost within the study area is continuous and ice-rich. The mean annual ground temperature (MAGT) at a depth of 10–15 m varies from −1.7 to −6.5 °C.

## 3. Methods

### 3.1. Sampling

Three boreholes (№ 12, 17 and 42) were drilled within the Holocene lagoon-marine floodplain of Ob Bay and the first lagoon-marine terrace near the Sabettayakha River mouth in winter 2014 using a light portable drill (Fig. 2). The drilling retrieved a 12 cm diameter core in an almost undisturbed condition. Massive ice was sampled from these boreholes for isotope, chemical and palynologic analyses.

Fragments about 30 cm long of three ice cores were taken from each borehole, transported in frozen state to Moscow, and kept in a freezer (Fig. 3). Then they were subsampled at 1–2 cm intervals. Ice samples were melted just before chemical and isotopic analyses and kept in glass vial bottles.

### 3.2. Oxygen and hydrogen isotope ratios

Isotopic analyses were performed in the Stable Isotope Laboratory of the Geographical Department of Lomonosov Moscow State University using a mass spectrometer Finnigan Delta-V with the standard gas – bench option. International standards V-SMOW (Vienna Standard Mean Ocean Water), GISP (Greenland Ice Sheet Precipitation) and SLAP (Standard Light Antarctic Precipitation), as well as the laboratory's own standard – fresh snow of the Caucasus glacier Garabashi ($\delta^{18}O = -15.60‰$, $\delta^2H = -110.0‰$) were used for the measurements. The precision of the $\delta^{18}O$ and $\delta^2H$ measurements is 0.1 and 0.6‰, respectively.

Analysis of the $\delta^2H$ and $\delta^{18}O$ composition of ice commonly provides insight into the origin of ice bodies. The use of $d_{exc}$ to identify the origin of ground ice or derive evidence of secondary processes has been sparked by its recent use in ice studies, where, unlike $\delta^2H$ and $\delta^{18}O$, variations of $d_{exc}$ reflect changes in the sources of moisture. The value of $d_{exc}$, the difference between $\delta^2H$ and $8\delta^{18}O$ (Dansgaard, 1964), also varies substantially in Arctic regions.

### 3.3. Ion concentration

Cation and anion concentrations in the ice were measured, immediately after the ice melted, in the Chemical-Analytical Centre of the Geographical Department of Lomonosov Moscow State University by ion chromatography "Stayer" with a conductivity detector. The limit for chloride ions is considered 0.02 µg/mL. The accuracy and precision over a wide concentration range, and total uncertainty (including random and systematic errors reported at the 95% confidence level) of anion and cation determinations were further estimated and the values were found to be sufficient for analysis of the ice.

### 3.4. Pollen and spores

Ice samples collected at 3 cm intervals to provide detailed information about pollen and spores preserved within the ice. Volume of each sample measured to determine the pollen and spore concentrations per 1 litre. To exclude contamination of the sample surface by modern pollen and spores, every sample of the ice washed with meltwater obtained from partial melting of the same sample. After melting of the sample, the produced water placed in 300-ml high-density polyethylene bottles. Each sample bottle left for 24 hours before being separated into 100-ml plastic bottles for the different analyses. Residue from the bottom of the 300-ml bottle used for pollen analysis in order to obtain a sufficient concentration of pollen and spores. Sample processing for the palynologic analyses included KOH deflocculation, treatment with HF (except for the samples of pure ice without ground or low concentration of ground particles) and mounting of pollen samples in glycerine. To simplify the process and prevent pollen loss, the samples were not subjected to either acetolysis. Cytoplasm in the pollen grains is not chemically removed, which allowed us to separate fresh pollen grains and reworked ones. Pollen percentages calculate based on the total pollen and spore sum and the results were tabulated.

### 3.5. $^{14}C$ AMS dating

Radiocarbon dating by accelerator mass spectrometry (AMS) performed on one sample (Ox A) of detrital organic in microinclu-


**Fig. 3.** Types of Holocene massive ice on the coast of the Ob Bay, near the Sabetta settlement, northeast of the Yamal Peninsula: a – brown vertical layered ice consisting of alternating veins of ice and sediment 0.2–2 mm thick (borehole number 42); b – white transparent, horizontal layered ice (borehole number 17); c – brown, non-laminated ice, with an admixture of fine sediments (borehole number 12). Photograph by Yu.Vasil'chuk.

sions from brown, non-laminated ice. The reliability of the measurement depends mainly on the sample characteristics and the degree to which the carbon extracted is all of the same radiocarbon age. The age is reported is uncalibrated and given in radiocarbon years BP (Before Present - AD 1950), using the half-life of 5568 years. Isotopic fractionation has been corrected for using $\delta^{13}C$ values measured independently by AMS on a stable isotope mass spectrometer (to $\pm$0.3 per mil relative to VPDB).

## 4. Results

### 4.1. Cryostratigraphy

Massive ground ice occurs in 43 locations (Fig. 4) from 51 boreholes drilled by Yamal LNG (liquefied natural gas) project, Arctic and Antarctic Research Institute, Center Hydroecological Research. The massive-ice bodies are located mainly in the Holocene deposits of lagoon-marine origin within lowered remnants of the first terrace and lagoon-marine floodplain of Ob Bay. The bodies occur at different depths, forming sometimes a two- to four-stage complex.

The massive-ice bodies occur as more or less homogeneous layers that vary in thickness from a few centimeters to a few meters and extend horizontally for up to tens of meters. Their top lies at a depth of 0.6 to 21.1 m, and their bottom at a depth of 1.6 to 21.4 m. The thickness of ice in boreholes ranges from 0.2 to 5.7 m (average = 1.5 m). In some cases, two and three horizons of ice revealed in individual boreholes (Figs. 4 and 5). The ice is mainly fresh, similar to lake and meteoric water. Massive-ice bodies occur in sandy-clay, sand and clay and are often confined to the contact between different sediment textures. In 60% of cases, however, the massive ice occurs in sandy sediments. Massive-ice bodies are commonly overlain by sand (59% of cases), sandy loam (25%) and loam (11%); and underlain by sand (58%), sandy loam (26%) and loam (15%). Peat overlies 4% of massive-ice bodies and underlies 0.3% of them. Some massive-ice bodies occur in the bottom lake sediments (Fig. 5, d, e).

Massive-ice bodies in floodplain deposits have different lateral extents. The lateral extent of the lowest ice body may exceed 50 m (Fig. 4, a, c, d; 5 a-c). The massive-ice bodies are usually underlain by sand, but in some cases, they are underlain by a thin loam and sandy loam horizon (Fig. 4, b, d; 5d, borehole 66). Borehole 66 revealed three layers of massive ice about 1 m thick at depths of 2, 4 and 8 m. The lateral extent of massive-ice bodies in the first terrace deposits apparently exceeds 50 m (Fig. 5f, g) and their thickness exceeds 2 m. Such ice bodies protrude into floodplain deposits. In some cases, ice wedges penetrate the uppermost massive-ice bodies.

### 4.2. Massive ice

Three types of massive ice are described in detail from boreholes 12, 17 and 42. The first, brown vertical layered ice consisting of alternating veins of ice and sediment 0.2–2 mm thick was observed in the upper part of borehole № 42 (Fig. 2c). The mineral sediment content of the ice estimates at up to 6–8% by volume. The second, white transparent, horizontal layered ice is observed in the lower part of borehole №17 (Fig. 2b). The third, brown, non-laminated ice with an admixture of fine sediments occurs in the neighboring borehole № 12 (Fig. 2a). In the upper part of the section brown ice both with and without vertical lamination occurs, which may to indicate a single source of water, but different freezing conditions.

#### 4.2.1. $^{14}C$ age of massive ice

Organic material in microinclusions from brown, non-laminated ice (borehole № 12, 6.8 m depth) was submitted for dating to the AMS laboratories at Oxford University. A $^{14}C$ age of 5932 ± 39 years BP (OxA-X-2650-57) was obtained. The calibrated $^{14}C$ age of the Sabetta brown, non-laminated ice is 4931–4717 cal BC (supplementary material Fig. S5). (IntCal 13 calibration curve) [3]. The $\delta^{13}C$ value of the sample is −29.44‰.

#### 4.2.2. Oxygen and hydrogen isotope ratios of massive ice

Deuterium and heavy oxygen isotope analyses carried out on samples of the three types of massive ice (Fig. 3). In brown vertical non-laminated ice from the borehole № 12, $\delta^2H$ values range from −147.62 to −155.57 ‰, and $\delta^{18}O$ values range from −19.11 to −20.55 ‰. In white horizontal layered ice from borehole № 17, $\delta^2H$

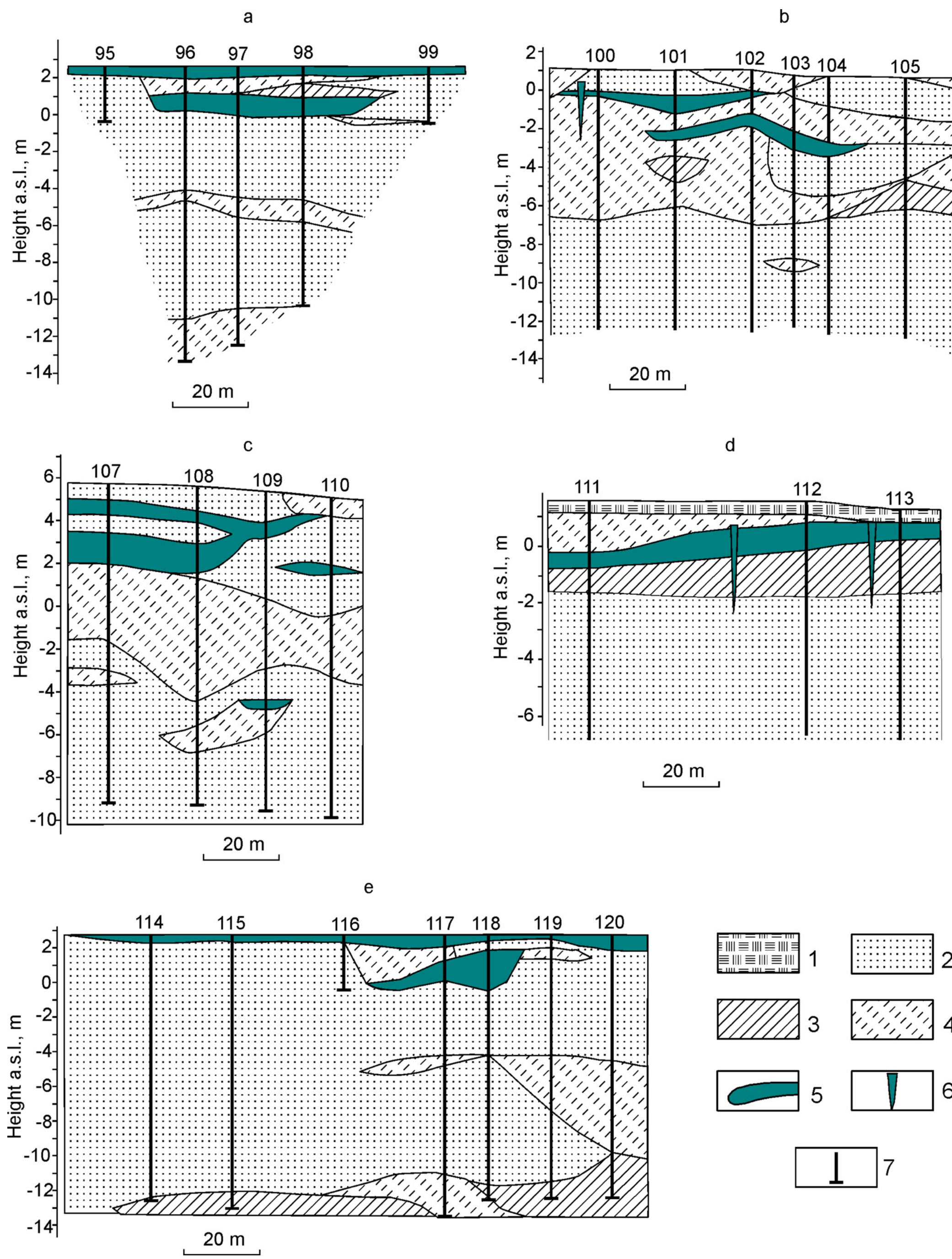


**Fig. 4.** Multistage massive ice revealed by new boreholes on the coast of Ob Bay near Sabetta settlement, northeast Yamal Peninsula: 1 – moss and plant cover; 2 – sand; 3 – loam; 4 – sandy loam; 5 – massive-ice bodies; 6 – ice wedges; 7 – boreholes and their numbers.

values range from −107.1 to −119.8 ‰, and $\delta^{18}$O values range from −15.73 to −16.06 ‰. Brown vertical layered ice with an admixture of mineral sediments from the borehole № 42 is characterized by extremely low values of $\delta^2$H, from −194.5 to −199.7 ‰, and $\delta^{18}$O values range from −25.33 to −26.48 ‰ (Table 1).

The $\delta^{18}$O – $\delta^2$H diagram for brown vertical layered ice from the borehole № 42 does not show a linear trend, because all values are clustered ($\delta^{18}$O from −26.5 to 25.33‰, $\delta^2$H from −199.7 to −192.7‰) (Fig. 6). Such negative values are more consistent with ice-wedge ice and massive ice of Late Pleistocene age than Holocene age. Nevertheless, taking into account the Holocene age of the sediments surrounding the massive ice, this may indicate either intrasedimental formation of the ice body during stable conditions with equilibrium isotope fractionation or burial of floes of river ice.

*4.2.3. Chemical composition of massive ice*

The salinity of ice varies markedly from 10.92 to 229.28 mg/l (supplementary material Table S1). Chloride prevails in all types of ice.

The brown vertical layered ice is ultra-fresh, with a salinity value of 40.64 mg/l, a chloride value of 34.53%-equivalent, sulfate of 35.92%-equivalent, magnesium of 51.37%-equivalent), and a pH of 7.9. The bicarbonate content is 29.14%-equivalent, which may be

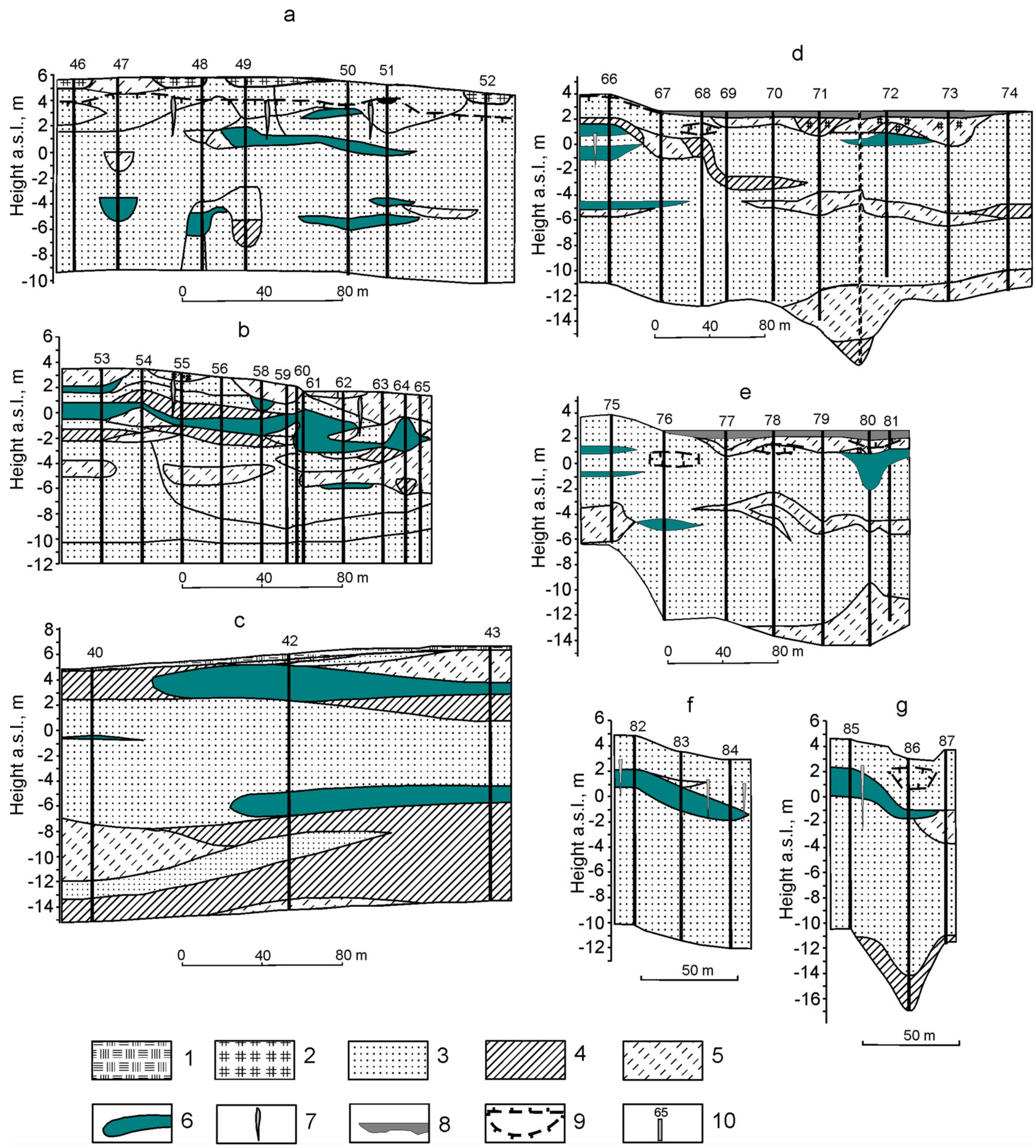


**Fig. 5.** Permafrost sediments and multistage massive-ice bodies revealed by boreholes on the coast of Ob Bay near Sabetta settlement, northeast Yamal Peninsula (modified from [43, 44]): 1 – moss and plant cover; 2 – peat; 3 – sand; 4 – loam 5 – sandy loam; 6 – massive-ice bodies; 7 – ice wedges; 8 – lake ice; 9 – permafrost; 10 – boreholes and their numbers.

explained by gradual freezing of host sand. The $Cl^-/SO_4^{2-}$ ratio is 0.96 (Table S1), which is close to that of the Ob Bay water (0.84%-equivalent) [6].

The white horizontal layered ice is characterized by the lowest salinity (10.92–13.52 mg/l), magnesium chloride and calcium chloride ions and a pH of 8. The $Cl^-/SO_4^{2-}$ ratio ranges from 3.29 to 4.95, similar to values obtained by Fotiev [6] for texture ice (4.30) and river water (4.67).

The brown, non-laminated ice has a salinity of 81.9 mg/l and comprises sodium chloride, a pH of 7.5, and a $Cl^-/SO_4^{2-}$ ratio of 9.77. The chemical composition of this ice is close to that of fresh massive-ice bodies of Yamal Peninsula [34]. Another sample of brown, non-laminated ice has a salinity of 229.28 mg/l, comprises sodium chloride, with a pH of 6.7. The rather high $Cl^-/SO_4^{2-}$ ratio (68.91) is explained by a low concentration of sulfates, which is usual for cryopegs (i.e. a layer of unfrozen ground at temperatures below 0 °C), particularly under river channels.

The concentration of dissolved ions in brown non-laminated ice is high (233.0–661.01 µS/cm) in comparison with that of brown vertical layered ice (102.5 µS/cm) and white horizontal layered ice (13.5–18.98 µS/cm). Ion concentrations in all types of studied ice are similar to those of meteoric and fresh surface waters, for example snow sampled in Moscow and lake ice on Baikal Lake (15.45–203 and 25.6 µS/cm, respectively).

### 4.2.4. Pollen analysis of massive ice

Pollen concentrations in massive ice at the mouth of the Sabettayakha River are low (no more than 360 grains/l), and some horizons lack pollen and spores (supplementary material Table S2, № 2–4). We used pollen analysis for the additional indication of the origin of the ice, therefore it was important, both every pollen grain and pollen spectra in general.

Pollen spectra from massive ice at Sabetta generally correspond to those of present-day Arctic tundra landscapes. We compare the

**Table 1**
$\delta^2H$, $\delta^{18}O$ and $d_{exc}$ values in Holocene massive ice near Sabettayakha River mouth.

| № | $\delta^2H$, ‰ | $\delta^{18}O$, ‰ | $d_{exc}$, ‰ | № | $\delta^2H$, ‰ | $\delta^{18}O$, ‰ | $d_{exc}$, ‰ |
|---|---|---|---|---|---|---|---|
| *Borehole 12, depth 6.5–6.8 m, brown non-laminated ice* | | | | *Borehole 42, depth 1.3–1.6 m, brown vertical layered ice* | | | |
| 12/1 | −150.39 | −19.98 | 9.45 | 42/8 | −197.6 | −26.07 | 10.96 |
| 12/2 | −147.62 | −19.11 | 5.26 | 42/9 | −194.8 | −25.92 | 12.56 |
| 12/3 | −152.8 | −20.21 | 8.88 | 42/10 | −194.7 | −25.76 | 11.38 |
| 12/4 | −155.57 | −20.19 | 5.95 | 42/11 | −193.4 | −26.04 | 14.92 |
| 12/5 | −151.77 | −20.55 | 12.63 | 42/12 | −192.7 | −25.33 | 9.94 |
| 12/6 | −149.7 | −20.22 | 12.06 | 42/18 | −193.8 | −26.24 | 16.12 |
| 12/7 | −154.53 | −20.18 | 6.91 | 42/19 | −196.5 | −26.12 | 12.46 |
| *Borehole 17, depth 8.3–8.5 m, white transparent. horizontal layered ice* | | | | 42/20 | −198.5 | −26.46 | 13.18 |
| 17/13 | −107.1 | −15.77 | 19.09 | 42/21 | −197.2 | −26.25 | 12.8 |
| 17/14 | −110.5 | −15.79 | 15.8 | 42/22 | −198.3 | −26.12 | 10.66 |
| 17/15 | −114.2 | −16.02 | 13.87 | 42/23 | −197.2 | −26.01 | 10.88 |
| 17/16 | −113.5 | −16.06 | 14.90 | 42/24 | −194.5 | −25.65 | 10.7 |
| 17/17 | −114.9 | −15.74 | 10.96 | 42/25 | −194.5 | −26.07 | 14.06 |
| 17/32 | −115.3 | −15.89 | 11.83 | 42/26 | −196.2 | −26.24 | 13.72 |
| 17/33 | −112.5 | −15.87 | 14.46 | 42/27 | −199.3 | −26.23 | 10.54 |
| 17/34 | −119.8 | −15.73 | 6.01 | 42/28 | −198.6 | −26.36 | 12.28 |
| 17/35 | −118.8 | −15.80 | 7.62 | 42/29 | −199.7 | −26.28 | 10.54 |
| 17/36 | −113.2 | −15.57 | 11.36 | 42/30 | −197.2 | −26.48 | 14.64 |
| 17/37 | −112.9 | −15.62 | 12.11 | 42/31 | −199.7 | −25.98 | 8.14 |

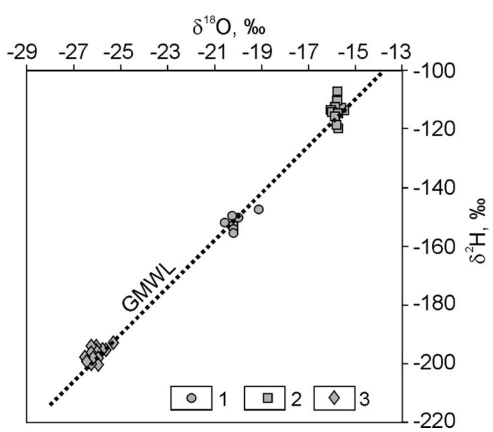


**Fig. 6.** $\delta^{18}O$-$\delta^2H$ plot of the three types massive ice at Sabetta. V-SMOW, Vienna Standard Mean Ocean Water; GMWL, Global Meteoric Water Line. 1 – brown, non-laminated ice, with an admixture of fine sediments; 2 – white transparent, horizontal layered ice; 3 – brown vertical layered ice consisting of alternating veins of ice and sediment 0.2–2 mm thick.

Sabetta pollen spectra with those from massive ice elsewhere in this region (see Fig. 1): at Kharasavey Cape (Table S2, № 6), near the Upper Mordyyakha River (№ 7), and near the mouth of the Gyda River (№ 8). We also compare them with typical pollen spectra from snow patch at Matuysale (№ 9) and near the Gyda River mouth (№ 10), with an ice floe (sea ice) in Gyda Bay (№ 11), from Late Holocene ice-wedge ice near the Tambey River mouth, 13 km to north of Sabetta (№12) and from Holocene ice wedges at Matuysale, near the mouth of the Salemlekamtambda River (Table S2, № 13).

Given the $\delta^{18}O$ values of −26‰ from the massive ice, we need to compare the pollen spectra from such massive ice with pollen spectra from Late Pleistocene ice-wedge ice. It may be possible to compare them with pollen spectra Late Pleistocene ice-wedge ice near Seyakha settlement (about 80 km to the south), from which pollen concentrate has been $^{14}C$ dated by AMS to 25–21 kyr BP [33,39]. Far-transported pollen consists of 12–17% of the total sum (*Picea* sp. 1–2%, *Pinus sylvestris* 3–5%, *P. sibirica* 3–6%, *Betula* sect *Albae* 4–6%, *Alnus* sp.1%), which is more than in the pollen spectra of the massive ice studied, but less than in pollen spectra of Holocene ice wedges in Tambey river valley. Percentages of shrub pollen (15–30%) are similar to the pollen spectra of massive ice. The variety of local herb pollen in the Late Pleistocene ice wedges surpasses that in massive ice: Caryophyllaceae, Ericaceae, Papaveraceae, *Polygonum bistorta*, Liliaceae, *Sparganium*, which is typical of Late Pleistocene vegetation. Thus, pollen spectra of brown vertically layered ice differ from those of Late Pleistocene ice wedges.

The key difference in terms of pollen spectra between massive-ice samples in this area is the predominance of shrub pollen at Sabetta. Massive ice at Sabetta contains 32–53% shrub pollen, compared to 36–43% in massive ice elsewhere on the Yamal Peninsula (e.g. near Kharasavey settlement and in the Mordyyakha River valley), and on the Gydan Peninsula (near the Gyda River mouth). Brown vertical layered ice from borehole № 42 is characterized by a prevalence of pollen of *Betula* sect. *Nanae, Alnaster* sp., Cyperaceae, *Equisetum*, and Bryales.

The real origin of "Bryales" spores is uncertain, and we understand "Bryales" to represent transparent small, round cells often with spines about 10–20 µm in diameter. Most of the pollen and spores are poorly preserved; they are often enveloped by clay particles and probably derived from the host sediment. These pollen spectra are similar to those of Holocene floodplains of this area (Vasil'chuk, 2005), and therefore we suggest that the massive-ice body formed during the Holocene. The white horizontally layered ice from the borehole № 17 (Table S2, № 3–5) is characterized by low pollen concentrations, a predominance of shrub pollen and a noticeable amount of Cyperaceae pollen. Sample №3 (Table S2) contains perfectly preserved pollen of *Betula* sect.*Nanae*, which had been incorporated into the ice without any reworking. The presence of rounded quartz grains in the 10–60 µm fraction may indicate water transport. Remains of the seaweed *Pediastrum*, coal particles, and fungal spores also are also found in vertical layered brown ice and in white massive ice.

### 4.3. Cryopegs

Cryopegs in the permafrost have been identified in 4 boreholes (see supplementary Fig. S6 for more details). Cryopegs occur most often in saline permafrost developed within fine-grained sands at different depths and as lenses of different thickness. Pressure and salinity of cryopeg lenses are different, which indicates the absence of hydraulic connection between them. Additionally, the lateral extent of the cryopeg lenses is often less than the distance between the boreholes. The composition of brines comprises magnesium chloride and sodium chloride, with a salinity of 62.35–93.10 g/l and a temperature of −5.2 to −5.6 °C.

## 5. Discussion

### 5.1. Heterogeneity of massive-ice bodies

Two prominent features of Holocene massive-ice bodies at the mouth of the Sabettayakha River are 1) the combination of different types of ice (white horizontal layered ice, brown non-laminated ice and brown vertical layered ice) and 2) the considerable contrast of isotope values of different types of ice (>10‰ for $\delta^{18}$O and > 90‰ for $\delta^{2}$H).

Analysis of the $\delta^{2}$H and $\delta^{18}$O composition of ice commonly provides insight into the origin of ice bodies [2,7–9, 27,29,32,36]. The use of $d_{exc}$, the difference between $\delta^{2}$H and 8$\delta^{18}$O, to identify the origin of ground ice or derive evidence of secondary processes has been sparked by its recent use in ice studies, where, unlike $\delta^{2}$H and $\delta^{18}$O, variations of $d_{exc}$ reflect changes in the sources of moisture.

*Brown vertical layered ice.* The very negative isotope values in brown vertical layered ice ($\delta^{2}$H from −194.5 to −199.7 ‰, and $\delta^{18}$O from −25.33 to −26.48 ‰) might be explained by burial of strongly deformed glacial ice of Late Pleistocene age. Vertical lamination within massive-ice bodies of Yamal Peninsula is not rare, and Vasil'chuk et al. (2009, [34,42]) noted vertical lamination in the Late Pleistocene massive ice near Bovanenkovo gas field, in the valleys of Erkutayakha River and Mordyyakha River, in the upper part of the section at Marre-Sale [23]. However, these massive-ice bodies often contain remains of seaweed and characterized by tundra pollen spectra that exclude a glacial origin (Vasil'chuk et al., 2009, [42]). We suppose that a glacial origin is also excluded for vertical layered ice in lagoon-marine Holocene sediments near the Sabettayakha River mouth. More generally, if the host sediments are of Holocene age, as inferred above, and the Yamal Peninsula was last glaciated during the early Weichselian [1,5], then a buried glacier origin can be discounted.

The vertical layering of massive ice in Late Pleistocene and Holocene sediments may result from both primary and secondary folding. Secondary deformation occurs, for example, when a moving glacier deforms horizontally-layered massive ice or where ice wedges penetrate horizontally-layered massive from the top, which locally reduces the overburden weight (because ice is less dense than mineral soil) and allows the massive ice to arch upwards. Secondary deformation may also result when injection ice (water) intruded into it from the bottom and bended the ice layers upwards. A combination of autochthonous and allochthonous massive-ice bodies is observed in the upper Yuribey River in Yamal Peninsula. Initially horizontal massive ice 2.0–3.0 m thick was folded upward by injection of pressurized water from the bottom and its freezing to form a body of injection ice (> 4 m in vertical dimension) [34]. Similarly, the combination of two different types of massive ice investigated in Erkutayakha River valley [42], where initially horizontally layered segregated ice (primary vertical thickness of about 4 m) is deformed by intrusion of injected ice from the bottom. Its size is about 10 m vertically and over 25 m horizontally. An example of a folded massive-ice body at Herschel Island, western Arctic Canada, demonstrates vertical layering [7,18]. The horizontal layers of the ice are replaced by inclined and vertical ones along the fold (see supplementary Fig. S7a for visual comparison). Without discussing here the origin of this deformation, we note that at the case of drilling the well at the point of limb of the fold the resulting core may to contain vertically layered ice (Fig. S7c).

Particular attention was paid to vertical layered ice in the upper parts of some boreholes, because its position near to the surface may point to an origin as ice-wedge ice. This interpretation is consistent with the similarity of the ice to alternating veins of ice and sand within composite wedges formed by infilling of thermal contraction cracks with ice, sand or ice-sand mixtures in the Summer Island area of the Tuktoyaktuk Coastlands, western Arctic Canada (supplementary Fig. S7b; [13]). However, according to personal communication of V. Rogov (Moscow State University, Department of Cryolithology and Glaciology) the brown vertical layered ice is not ice-wedge ice (Fig. S4). Alternatively, if the vertical layered ice represents an ice dyke, it should have smaller ice crystals along each margin [11], which we did not observe.

Perhaps an additional indication of ice genesis is the isotopic contrast of ice within a single ice body, especially when the isotope range exceeds 4–5 ‰ for $\delta^{18}$O and 30–40 ‰ for $\delta^{2}$H. As noted earlier, the range of isotope values of vertical layered ice and underlying white ice is 10‰ for $\delta^{18}$O and almost 90‰ for $\delta_D$ (Fig. 7a). We obtained a much larger isotope range (18‰ for $\delta^{18}$O) in the uniform lenses of intrasedimental ice body in the Gyda River mouth, Gydan Peninsula (Fig. 7b; [36]) that is caused by cryogenic fractionation during freezing of water-saturated alluvial sediments in a closed system without water recharge.

The very negative isotope values ($\delta^{2}$H up to −199.7‰, $\delta^{18}$O up to −26.48‰) in brown vertical layered ice are unique not only for Holocene ground ice of the Yamal Peninsula but also for Late Pleistocene ground ice of northwest Siberia ([38]; Vasil' chuk, [41]). Ice wedges of Late Pleistocene age near Seyaha settlement on the eastern coast of Yamal Peninsula formed from winter snow and are characterized by $\delta^{18}$O values that are isotopically heavier than −25‰ and $\delta^{2}$H values not lower −189‰ ([36], 2006).

Late Pleistocene massive-ice bodies are characterized by $\delta^{18}$O values of −19.24 to −23.42‰ and by $\delta^{2}$H from −149.6 to −172.7‰ in the Erkutayakha River valley [42]; $\delta^{18}$O values of −21 to −23.3‰ and $\delta^{2}$H values of −164.8 to −172.9‰ in the Mordyyakha River valley (Vasil' chuk et al., 2012); and $\delta^{18}$O values of −12.49 to −23.13‰ and $\delta^{2}$H values of −91.7 to −177.1‰ in the Bovanenkovo gas field (Vasil' chuk et al., 2009; [41]). Isotope signatures of Pleistocene massive-ice bodies on the Yamal and Gydan peninsulas are rather negative [2,37,41]: the minimum values are −197.5‰ for $\delta^{2}$H and −26.26‰ for $\delta^{18}$O near Kharasavey Cape; −163.6‰ $\delta^{2}$H and −25.5‰ $\delta^{18}$O in the Oyuyaha River valley; and −190.6‰ $\delta^{2}$H and −24.8‰ $\delta^{18}$O near Marre-Sale station [23,27]. The unusually variable isotope values of the massive-ice bodies in the Sabettayakha River mouth are likely to be a result of cryogenic fractionation during freezing, which indicates a mainly intrasedimental segregated or segregated-infiltrated genesis. However, we do not exclude the possibility that different types of water such as that from winter precipitation with extremely negative values have contributed to the formation of brown vertical layered ice, and lake waters may have contributed to the formation of white and brown ice. We also do not exclude a buried genesis of individual layers because of catastrophic burial of ice floes and ice feet (derived from isotope depleted winter snow). Such burial could result from the spring congestion and pile-up of sea ice in Ob Bay, which transported a considerable mass of sand.

The chemical composition of the brown vertical layered ice suggests that it formed during freezing of sand saturated by Ob Bay waters.

Most pollen grains and spores within this ice have clay envelopes, which may indicate that they are derived from the host sediments. The presence of *Equisetum* spores along with Cyperaceae pollen in brown vertical layered ice may indicate a lacustrine-paludal origin of water from a sublake talik. Holocene ice wedges in floodplain sediment near Sabetta settlement in the Tambey River mouth area (Table S2, № 12) are characterized by high percentages of *Pinus* and *Picea* pollen (40%) [43] and their pollen spectra differ from those from massive ice in Sabetta. The difference is caused by peculiarities in pollen accumulation. In terms of ice wedges, the pollen and spores transported by wind on the snow cover and, together with snow meltwater, enter frost

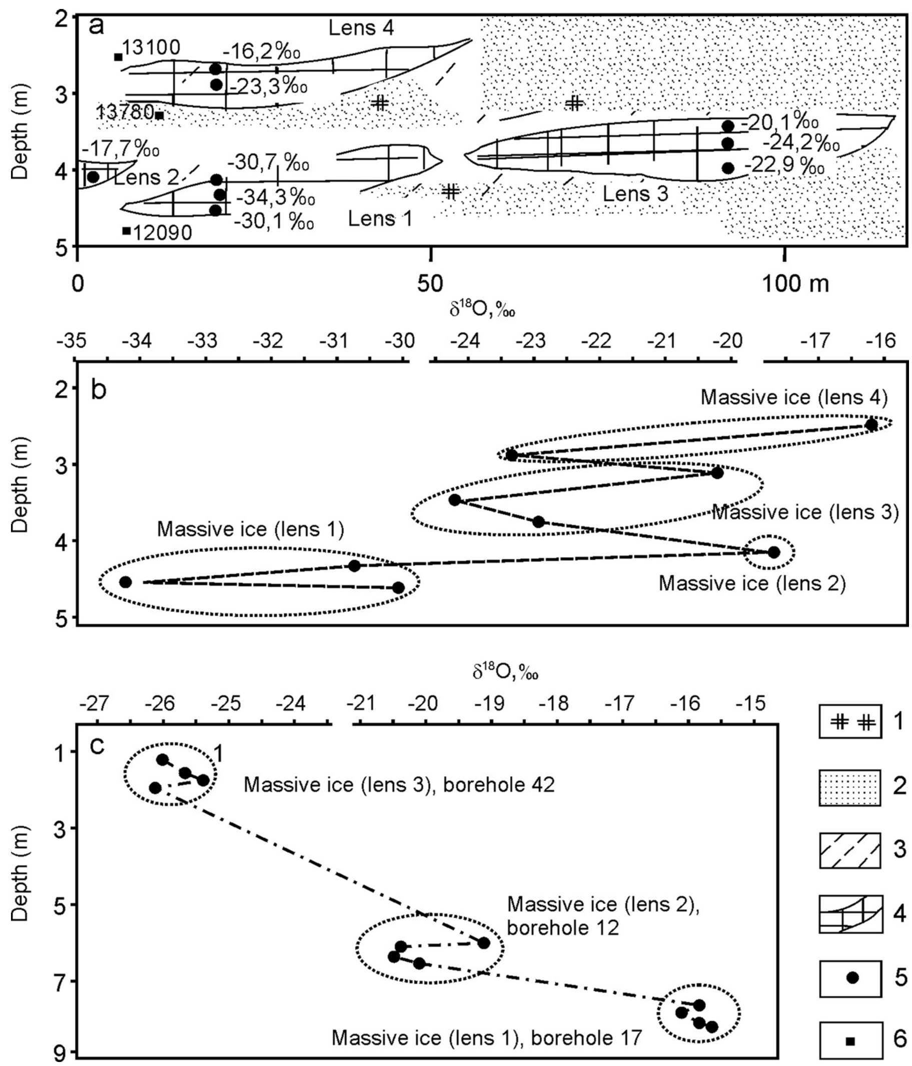


**Fig. 7.** Contrasting $\delta^{18}O$ values in (a) multiple lenses of segregation ice within the first alluvial terrace near the mouth Gyda River, north Gydan Peninsula; (b) four ice lenses and their comparison with contrasting $\delta^{18}O$ values in the four ice lenses (c) formed in Holocene sediments within the floodplain and first lagoon-marine terrace at the mouth Sabettayakha River: 1 – allochthonous peat and scattered detritus; 2 – sand; 3 – sandy loam; 4 – segregated ice; and sample points for: 5 – oxygen isotopic analysis, and 6 – on radiocarbon analysis.

cracks that penetrate the ice wedges. The wedge ice may therefore contain pollen and spores of regional derivation, including wind-transported pollen of Poaceae, Cyperaceae, Ericaceae, *Artemisia* and also *Pinus* and *Picea* (Table S2, № 12). In contrast, intrasedimental massive ice may contain that pollen and spores which derived from the host sediment and transported to the ice by flowing groundwater. Thus, pollen spectra from vertically layered brown ice do not give reasons for attributing it to Holocene ice-wedge ice.

Pollen data also suggest that an origin of the vertical layered massive ice as either buried snow or buried ice floe is unlikely. Herb pollen often accumulates on a surface of snow patch because the pollen of the local plants is transported there in summer (Table S2, № 9, 10). Because no herb pollen was found in the massive ice at Sabetta (Table S2, № 1–5), we conclude that this ice is not a buried snow patch. The pollen spectra of ice floes are often similar to those of ice wedges because the regional pollen and spores are mainly wind-transported, and far-transported tree pollen is often found at the surface of floes. Pollen spectra of sea-ice and snow samples near the North Pole show a dominance of trees and shrubs (89–93%), including pollen of broad-leaved trees such as *Quercus robur, Ilex aquifolium, Ulmus glabra, Tilia* sp. [31]. But, pollen of broad-leaved trees is not found in the massive ice in Sabetta, and so we believe that buried ice floes are unlikely to account for its origin.

The presence of seaweed suggests that ice formed during freezing of sublake taliks or bottom sediments of the Ob Bay. Similar pollen spectra obtained for the multilayered massive ice body in the Gyda River mouth (Table S2, № 8) [34].

*White transparent, horizontal layered ice.* This ice is characterized by low salinity. Its chemical composition is similar to the average chemical composition of river water in Yamal Peninsula [6], and the $Cl^-/SO_4^{2-}$ ratio values are within the limits of those in river or texture ice. Rounded quartz grains in the 10–60 µm fraction are abundant in the ice, which may indicate their transfer by water. Pollen spectra in this massive ice are characterized by their sparseness and prevailing NAP pollen of *Alnaster* (16.1%), *Betula* sect. *Nanae* pollen (21.4%) and Cyperaceae (25.0%), and a total absence local herb pollen. Far-transported pollen of *Betula* is well preserved (7.1%). The presence of seaweed suggests that the ice may have formed during freezing of a talik that had developed beneath a river or lake.

*Brown, non-laminated ice.* The $^{14}C$ age of organic microinclusions in this ice is 4931–4717 cal BC. The salinity of the brown, non-laminated ice varies from 81.9 to 229.28 mg/l. The latter is due to presence of fine sediment. Fresh massive-ice bodies of Yamal Peninsula often have a similar salinity and ratio of $Cl^-/SO_4^{2-}$, due to low concentrations of sulfate ions, particularly. Aggradation of permafrost under river channels accompanied the formation of cryopegs and massive ice. The results of pollen analysis and the chemical composition suggest that massive ice in Sabetta formed during freezing of water-saturated sediments and is therefore of intrasedimental origin.

The geocryological and palaeogeographical characteristics of Holocene massive-ice bodies are valuable because their structure and fabric can be used as indicators for the study of Pleistocene massive ice of unknown genesis. The massive-ice bodies in Holocene sediments near Sabettayakha River mouth are heterogeneous and are thought to represent a complex of segregation and intrusive-segregation ice. However, we do not exclude a buried genesis of individual layers because of catastrophic burial of ice floes and ice feet, or bottom lake ice. The possible burial of ice floes in lacustrine depressions may indicate the vertical position of massive-ice layers.

### 5.2. Massive ice in holocene sediments

Although reports of Holocene massive ground ice are rare, there are several findings in northern Eurasia, Canada and Alaska with which to compare the massive ice from Sabetta.

A layer of tabular massive ice 4 m thick ice occurs in the first terrace exposure near the Kharasavey village, on the northwest coast of Yamal Peninsula (Fig. 1; [4]). The radiocarbon age of the bottom of the first terrace at this site is about 9 kyr BP [36]. The salinity of the ice varies in the range of 10–90 mg/l, the $\delta^{18}O$ value (Fig. 8a) is −10.6 ‰, and $\delta^2H$ is −112 ‰. This ice is isotopically heavier than Holocene ice wedges near Kharasavey ($\delta^{18}O$ – 15.9 to −14.1 ‰) [36]. The massive ice probably formed in the Holocene. According to its isotopic signature, this massive ice segregated from mixed summer and winter water, and so there is no reason to believe that it is buried ice floe [34,37].

Massive ice 15 m thick and at a depth of about 4–6 m, identified from ground penetrating radar and electrical resistivity tomography data (Olenchenko and Shein, 2012), underlies an old channel of the Yuribey River (Yamal Peninsula), about 40 km upstream of its mouth (Fig. 8b). The massive ice is thought to have formed by freezing of a talik beneath the river.

Massive ice 1.2 m thick within sand has been identified in boreholes beneath a coastal bar 1–3 m a.s.l. at the shore of the Pechora Sea [45]. The top of the ice was at a depth of 0.6–1.1 m below the surface and aligned parallel to the surface topography (Fig. 8c). Beneath the ice was a cryopeg (up to 7 m thick) in the sand and a boulder clay loam. The ice has been interpreted as segregated, homogenous and of Holocene age.

Massive ice beneath the floodplain at the confluence of rivers Naduy-Yakha and Seyaha has also been identified, in boreholes, at depths of 2 to 10 m and about 30 m from the surface [26]. Here, sandy marine sediments of Late Pleistocene age contained a cryopeg at about the same depth as the lower layer of massive ice.

In Arctic Canada, a massive-ice complex of Holocene age has been described from the western bank of Hot Weather Creek, Fosheim Peninsula, Ellesmere Island (79°58′ N, 84°28′ W, Fig. 8d; [22]). Three types of massive ice identified by these authors and interpreted as ice-wedge ice, segregated ice and intrusive ice. All of them formed during or just after the time when permafrost aggraded downward into silt and sand uplifted above sea level about 7 kyr BP. Nearby at Slider River, Eureka Sound, $\delta^{18}O$ values of −28.9 to −34.8 ‰ were obtained from reticulate ice in fine-grained marine sediments above the massive ice and $\delta^{18}O$ values of −33.0 to −36.8 ‰ from the massive ice itself (Fig. 8e; [19]). Such similar values suggest a common source of water, presumably atmospheric precipitation. The massive ice is interpreted as intrasedimental in origin, having formed as permafrost aggraded after the land started to emerge from the sea at about 8 kyr BP.

Holocene massive-ice bodies have also been observed in boreholes beneath the coastal zone or seabed offshore of the Russian Arctic coast. Massive ice 14 m thick is found in modern marine sediments in the tidal zone on the beach at Kozhevnikov Bay, near the mouth of Khatanga River (Fig. 7f; [20]). In addition, massive ice 10 m thick underlies the seabed beneath 13 m of seawater at Baidarata Bay, 12 km offshore (Fig. 8g; Melnikov and Spesivtsev, 1995), and massive ice about 6 m thick was revealed under the beach near Kharasavey (Fig. 8h; [10]).

Massive ice of presumed Holocene age has been detected beneath the northern shore of lake Elin, near the Yellow River, China (Fig. 8i; [46]). Permafrost sediments at a temperature of −0.65°C occurred at a depth of 3–16.5 m. A layer of pure fresh ice 4.45 m thick was found at a depth of 18.8–24.26 m. Its salinity did not exceed 0.02 g/l and its $\delta^{18}O$ values were −11.16 to −11.70‰ ($\delta^2H$ values from −77.9 to −83.2‰). Isotopic values of fresh ice are close to those of modern firn at this site. Cryopegs occurred above and below the ice layer, with salinities exceeding 10.0 g/l.

The massive-ice bodies within the Kara diamicton at Marre-Sale Cape (west Yamal Peninsula) have been interpreted for many years mainly as remnants of buried glacier ice [5]. The strata exposed along the coast are folded into a large, complex anticline with a northwest-southeast strike over 150–200 m in amplitude and a 15-km fold wavelength. In the center of this structure are abundant low-angle folds and other glaciotectonic structures. The age of the glaciation that deposited the Kara diamicton and buried within it bodies of glacier ice is thought to be > 40,000 yr BP [5]. However, the age and genesis of ground ice are still debated [23–25,27]. New radiocarbon dating of the deposits obtained by Opokina et al. [17] suggests that the age of the upper part of the section is younger than 35,000 yr BP. Indeed, the new radiocarbon ages (Fig. 8j) suggest that the ice stocks and laccoliths probably formed within a relatively short period from 5.7 to 3.7 ka BP [17].

## 6. Conclusions

1. Single or multiple bodies of massive ice occur at different depths within Holocene deposits of lagoon-marine origin near the Sabettayakha River mouth, on the eastern Yamal Peninsula of northwest Siberia. The top of massive-ice bodies lies at a depth of 0.6 to 21.1 m, and the bottom at a depth of 1.6 to 21.4 m. The thickness of ice ranges from 0.2 to 5.7 m, and the lateral extent may exceed 50 m.
2. Three types of massive ice are identified: (1) brown vertical layered ice consisting of alternating veins of ice and sediment 0.2–2 mm thick; (2) white transparent, horizontal layered ice; and (3) brown, non-laminated ice with an admixture of fine sediments.
3. Cryopegs occur at several depths, and have a salinity of up to 93 mg/l.
4. Stable isotope values of the massive-ice bodies are highly variable: $\delta^2H$ values vary from −107 to −199.7‰, and $\delta^{18}O$ from −15.7 to −26.48‰. They are attributed to cryogenic fractionation during freezing and are thought to indicate that the ice is mainly intrasedimental in origin. The most negative isotope values are lower than those in Late Pleistocene ice wedges of the Yamal Peninsula.

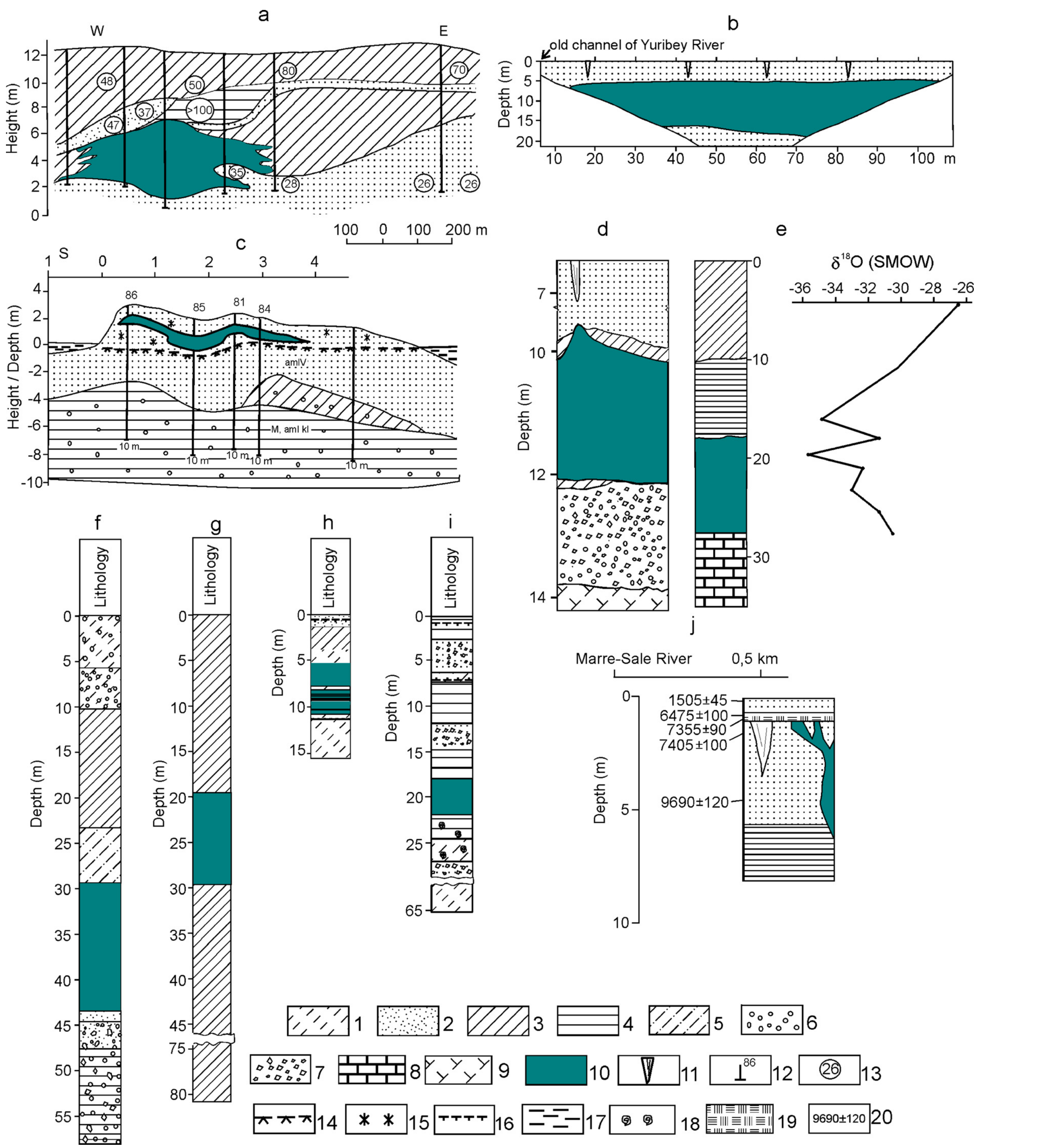


**Fig. 8.** a-c: homogenous massive-ice bodies in Holocene floodplain and marine (beach) sediments: a – massive-ice body 6 m thick in Holocene marine sediments near Kharasavey settlement (from [4]); b – floodplain sediments of Yuribey River (western Yamal Peninsula) with massive-ice bodies about 15 m thick [16]; c – modern segregated massive-ice body more than 1 m thick in the sediments of a sea bar of Russkiy Zavorot Peninsula (from [45]); d, e – intrasedimental massive-ice bodies underlain by pre-Quaternary rocks on the Fosheim Peninsula, Ellesmere Island, Canada: d – cryostratigraphy of the upper part of the cross-section at the Hot Weather Creek study site (from [22]); e – a stratigraphic column and $\delta^{18}O$ profile for a site near Slidre River, Eureka Sound, Canada (from [19]); f–i – Holocene massive-ice bodies revealed by boreholes in subaqueous conditions (f-h) and in lacustrine-alluvial deposits (i): f – borehole, revealed the massive-ice body 14 m thick in modern marine sediments in the tide zone on the beach at Kozhevnikov Bay, near the mouth of Khatanga River, Russian Arctic coast (from [20]); g – stratigraphy of the sediments in the borehole №240 drilled in subaqueous conditions of Baidarata Bay, 12 km off the coast, in a water depth of 13 m; the thickness of massive ice is 10 m (from [12]); h – stratigraphy of the sediments in the borehole №1 drilled in 1978 on the beach near Kharasavey revealed massive ice about 6 m thick (from [10]); i – stratigraphy and temperature in borehole №6 revealed massive ice 4.45 m thick on the north of Elin Lake, China (from [46]); j – massive ice near the cape Marre-Sale, western Yamal Peninsula (from [17]). 1 – sandy loam; 2 – sand; 3 – loam; 4 – clay; 5 – silty loam; 6 – pebble; 7 – gravel; 8 - weathered Tertiary sandstone; 9 – reworked Eureka Sound silt; 10 – massive ice; 11 – ice wedge; 12 – borehole location and number; 13 – moisture content (% dry weight); 14 – level of cryopegs; 15 – ice cement in sands above level of cryopegs; 16 – boundary of the permafrost; 17 – sea water; 18 – spiral fossils (gastropods, brackish species); 19 – peat; 20 – $^{14}C$ ages.

5. The chemical composition (especially the $Cl^-/SO_4^{2-}$ ratio) of the massive-ice bodies shows that brown vertical layered ice formed during freezing of sand saturated by Ob Bay waters; brown, non-laminated ice may have formed as a result of freezing of water-saturated sediment in a sublake talik; and white horizontal ultra-fresh layered ice could also be formed from river and lake water.
6. Pollen spectra support the intrasedimental interpretation of the massive-ice bodies. The presence of a seaweed remains within the ice suggests that ice was formed during freezing of sublake taliks or bottom sediments of the Ob Bay.


## Acknowledgements

Isotope research of YV, NB and JC is financially supported by the Russian Scientific Foundation (grant RSF No. 14-27-00083), and pollen research of AV is financially supported by a grant from the Russian Foundation for Basic Research (grant RFBR No. 14-05-00930). We are deeply indebted to Professor Julian Murton of the University of Sussex for his very careful and meticulous work in editing this manuscript.


## Supplementary materials

Supplementary material associated with this article can be found, in the online version, at doi:10.1016/j.grj.2016.09.002.

## References


[1] Astakhov V. The postglacial Pleistocene of the northern Russian mainland. Quater Sci Rev 2014;92:388–408. doi:10.1016/j.quascirev.2014.03.009.
[2] Belova NG. Massive ice beds of southwestern coast of the Kara Sea, Moscow: MAKS Press; 2014. (in Russian).
[3] Bronk Ramsay C, Scott EV, van der Plicht J. Calibration for archaeological and environmental terrestrial samples in the time range 26-50 cal BP. Radiocarbon 2013;55(4):2021–7. doi:10.2458/azu_js_rc.55.16935.
[4] Dubikov GI. Composition and cryogenic structure of permafrost in West Siberia, Moscow: GEOS Publisher; 2002. (In Russian).
[5] Forman SL, Ingólfsson Ó, Gataullin V, Manley W, Lokrantz H. Late quaternary stratigraphy, glacial limits, and Paleoenvironments of the Marresale Area, Western Yamal Peninsula, Russia. Quater Res 2002;57(3):355–70. doi:10.1006/qres.2002.2322.
[6] Fotiev SM. The regularities in the formation of natural waters of ionic-salt composition, Yamal Peninsula. Earth's Cryosphere 1999; 2(3): 40–65. (In Russian).
[7] Fritz M, Wetterich S, Meyer H, Schirrmeister L, Lantuit H, Pollard WH. Origin and characteristics of massive ground ice on Herschel Island (Western Canadian Arctic) as revealed by stable water Isotope and hydrochemical signatures. Permafrost Periglac Process 2011;22(1):26–38. doi:10.1002/ppp.714.
[8] Gibson J, Prowse T. Isotopic characteristics of ice cover in a large northern river basin. Hydrol Process 1999;13(16):2537–48 doi: 10.1002/(SICI)1099-1085(199911)13:16<2537::AID−HYP940>3.0.CO;2-A.
[9] Gibson J, Prowse T. Stable isotopes in river ice: identifying primary overwinter streamflow signals and their hydrological significance. Hydrol Process 2002;16(4):873–90. doi:10.1002/hyp.366.
[10] Grigoriev NF. Permafrost of the coastal area of Western Yamal Peninsula, Yakutsk: Siberian Branch of Russian Academy of Sciences Publ.; 1987. (in Russian).
[11] Mackay JR. Massive ice: some field criteria for the identification of ice types. In: Geological survey of Canada; 1989. p. 5–11. Current ResearchPaper 89-1G.
[12] Mel'nikov VP, Spesivtsev VI. Cryogenic formations in the earth's lithosphere, Novosibirsk: Siberian Publishing Center UIGGM, Siberian Branch of Russian Academy of Sciences; 2000. (in Russian and English).
[13] Murton JB. Morphology and paleoenvironmental significance of Quaternary sand veins, sand wedges, and composite wedges, Tuktoyaktuk Coastlands, Western Arctic Canada. J Sediment Res 1996;66(1):17–25. doi:10.1306/D4268298-2B26-11D7-8648000102C1865D.
[14] Murton JB. Ground-ice stratigraphy and formation at North Head, Tuktoyaktuk Coastlands, western Arctic Canada: a product of glacier–permafrost interactions. Permafrost Periglac Process 2005;16(1):31–50. doi:10.1002/ppp.513.
[15] Murton JB. Stratigraphy and palaeoenvironments of Richards Island and the eastern Beaufort Continental Shelf during the last glacial–interglacial cycle. Permafrost Periglac Process 2009;20(2):107–25. doi:10.1002/ppp.647.
[16] Olenchenko VV, Shein AN. Possibilities of geophysical methods in the search for Pleistocene megafauna in floodplain and above floodplain deposits of the Yuribey River (Yamal Peninsula). Earth's Cryosphere 2013;2(17):83–92 (in Russian).
[17] Opokina OL, Slagoda EA, Kurchatova AN. Stratigraphy of the section «Marre-Sale» (West Yamal Peninsula): analysis with consideration for new data on radiocarbon. Ice Snow 2015;4(55):87–94 (in Russian). doi:10.15356/2076-6734-2015-4-87-94.
[18] Pollard W. The nature and origin of ground ice in the Herschel Island area, Yukon Territory. In: Permafrost – Canada. Proceedings of the fifth Canadian permafrost conference. collection Nordicana, N54. Centre d'etudes Nordiques. Quebec: Universite Laval. National Research Council of Canada; 1990. p. 23–30.
[19] Pollard W, Bell T. Massive ice formation in the Eureka Sound Lowlands: a landscape model. In: Lewkowicz AG, Allard M, editors. Québec: Université Laval, N57. Yellowknife. Canada: Collection Nordicana, Canada; 1998. p. 903–8.
[20] Ponomarev VM. Formation of permafrost rocks and groundwater in the northern shallow sea. In: Physical and chemical processes in freezing and frozen rocks. Leningrad: Academy of Science of the USSR Publisher; 1961. p. 95–101.
[21] M Premke-Kraus. Holocene environmental history of the Kara Sea (Siberian Arctic, Russia) inferred from marine palynological records. Univer. Bremen: Geowissenschaften, PhD thesis, 2008.
[22] Robinson S, Pollard W. Massive ground ice within Eureka sound bedrock, fosheim peninsula. In: Ellesmere Island NWT, Lewkowicz AG, Allard M, editors. Proceedings of the seventh international conference on permafrost, N57. Yellowknife. Canada. Québec: Université Laval, Collection Nordicana, Canada; 1998. p. 949–54.
[23] Slagoda EA, Opokina OL, Rogov VV, Kurchatova AN. Structure and genesis of the ground ice in the Neopleistocene-Holocene sediments of Marre-Sale Cape, Western Yamal Peninsula. Earth's Cryosphere 2012;2(16):9–22 (in Russian).
[24] Solomatin VI. Physics and geography of ground glaciation, Novosibirsk: Academic Publishing House "Geo"; 2013. (in Russian).
[25] Shpolyanskaya NA. Pleistocene-Holocene history of the development of the Russian Arctic permafrost zone due to "eyes" of ground ice, Moscow-Izhevsk: Institute of Computer Science; 2015. (in Russian).
[26] Streletskaya ID, Leibman MO. Cryogeochemical interrelation of massive ground ice, cryopegs and enclosing deposits of Central Yamal. Earth's Cryosphere 2002;3(6):15–24 (in Russian).
[27] Streletskaya ID, Vasiliev AA, Oblogov GE, Matyukhin AG. Isotopic composition on ground ice in Western Yamal (Marre-Sale). Ice Snow 2013;2(122):83–92 (in Russian). doi:10.15356/2076-6734-2013-2-83-92.
[28] Svendsen JI, Alexanderson H, Astakhov VI, Demidov I, Dowdeswell JA, Funder S, et al. Late Quaternary ice sheet history of northern Eurasia. Quater Sci Rev 2004;23(11-13):1229–71. doi:10.1016/j.quascirev.2003.12.008.
[29] Swanger KM, Marchant DR, Kowalewski DE, Head III JW. Viscous flow lobes in central Taylor Valley, Antarctica: origin as remnant buried glacial ice. Geomorphology 2010;120:174–85.
[30] Trofimov VT, Badu YB, Dubikov GI. Cryogenic structure and iciness of permafrost of Western Siberia, Moscow: Moscow University Press; 1980. (in Russian).
[31] Ukraintseva VV, Sokolov VT. Pollen analysis of snow samples from the North Pole region. Polar Geogr 2003;27(3):268–71. doi:10.1080/789610182.
[32] Vaikmäe RA, Michel FA, Solomatin VI. Morphology, stratigraphy and oxygen isotope composition of fossil glacier ice at Ledyanaya Gora. Northwest Siberia, Russia. Boreas 1993;22(3):205–13. doi:10.1111/j.1502-3885.1993.tb00180.x.
[33] Vasil'chuk AC, Kim J-C, Vasil'chuk YK. The AMS dating of pollen from syngenetic ice-wedge ice. Nuc Instrum Methods Phys Res 2004;B 223–224:645–9. doi:10.1016/j.nimb.2004.04.119.
[34] Vasil'chuk AC, Vasil'chuk YK. Pollen and spores as massive ice origin indicators. In: Melnikov VP, Drozdov DD,, Romanovsky VE, editors. Proceedings of the tenth international conference on Permafrost, Salekhard, 25–29 June 2012. Salekhard: The Northern Publisher; 2012. p. 487–91.
[35] Vasil'chuk YK. Reconstruction of the paleoclimate of the late Pleistocene and Holocene on the basis of isotope studies of subsurface ice and waters of the permafrost zone. Water Resour 1991;17(6):640–7.
[36] Vasil'chuk YK. Oxygen isotope composition of ground ice. Application to palaeogeocryological reconstructions, 2-vols, Moscow: Geological Faculty of Moscow State University, Russian Academy of Sciences; 1992. (in Russian).
[37] Vasil'chuk YK. Stable isotope geochemistry of massive ice, Vol.1, Moscow: Moscow University Press; 2012. (in Russian).
[38] Vasil'chuk YK. Syngenetic ice wedges: cyclical formation, radiocarbon age and stable-isotope records. Permafrost Periglac Process 2013;24(1):82–93. doi:10.1002/ppp.1764.
[39] Vasil'chuk YK, van der Plicht J, Jungner H, Sonninen E, Vasil'chuk AC. First direct dating of Late Pleistocene ice-wedges by AMS. Earth Planet Sci Lett 2000;179(2):237–42. doi:10.1016/S0012-821X(00)00122-9.
[40] Vasil'chuk Y, Vasil'chuk A. Spatial distribution of mean winter air temperatures in Siberian permafrost at 20–18 ka BP using oxygen isotope data. Boreas 2014;43(3):678–87. doi:10.1111/bor.12033.
[41] Vasil'chuk YK, Vasil'chuk AC, Budantseva NA, Chizhova JN, Papesch W, Podborny YY. $^{14}C$ age, stable isotope composition and pollen analysis of massive ice, Bovanenkovo gas field, Central Yamal Peninsula. Geogr Environ Sustain 2014;2:49–70.
[42] Vasil'chuk YK, Budantseva NA, Vasil'chuk AC. Variations in $\delta^{18}O$, $\delta_D$, and the concentration of pollen and spores in an autochthonic heterogeneous massive ice on the Erkutayaha River in the southern part of the Yamal Peninsula. Doklady Earth Sci 2011;438(1):721–6. doi:10.1134/S1028334X11050382.
[43] Vasil'chuk YK, Budantseva NA, Vasil'chuk AC, Podborny YY, Sullina AN, Chizhova JN. Multistage holocene massive ice, Sabettayakha river mouth, Yamal Peninsula. Earth's Cryosphere 2015;4(19):48–60 (In Russian).

[44] Vasil'chuk YK, Budantseva NA, Vasil'chuk AC, Podborny YY, Chizhova JN. Holocene Massive Ice in north-west Siberia permafrost. Earth's Cryosphere 2016;1(20):36–50 (In Russian).

[45] Velikotsky MA. About massive ice in the sandy bars of the Pechora shore. In: Solomatin VI, editor. Problems of general and applied geo-ecology of the North. Moscow: Moscow University Press; 2001. p. 148–54. (in Russian).

[46] Wang S, Li W. First discovery of the deep-buried lake ice in source region of the yellow river. J Glaciol Geocryol 1990;12(3):201–7 (in Chinese).